

# Learning a Better Control Barrier Function

Bolun Dai<sup>1</sup>, Prashanth Krishnamurthy<sup>1</sup>, Farshad Khorrami<sup>1</sup>

**Abstract**— Control barrier functions (CBF) are widely used in safety-critical controllers. However, the construction of valid CBFs is well known to be challenging, especially for nonlinear or non-convex constraints and high relative degree systems. On the other hand, finding a conservative CBF that only recovers a portion of the true safe set is usually possible. In this work, starting from a “conservative” handcrafted control barrier function (HCBF), we develop a method to find a control barrier function that recovers a reasonably larger portion of the safe set. Using a different approach, by incorporating the hard constraints into an optimal control problem, e.g., MPC, we can safely generate solutions within the true safe set. Nevertheless, such an approach is usually computationally expensive and may not lend itself to real-time implementations. We propose to combine the two methods. During training, we utilize MPC to collect safe trajectory data. Thereafter, we train a neural network to estimate the difference between the HCBF and the CBF that recovers a closer solution to the true safe set. Using the proposed approach, we can generate a safe controller that is less conservative and computationally efficient. We validate our approach on three systems: a second-order integrator, ball-on-beam, and unicycle.

## I. INTRODUCTION

Safety is one of the most critical aspects when designing a controller [1]. With the integration of automated systems in our daily activities, e.g., self-driving cars [2] and robot manipulators [3], generating safe controls in unstructured environments has become increasingly important. Work has been done in generating safe trajectories using trajectory optimization [4]. However, safe controllers must be able to react to changing situations quickly, which requires the computational cost to be small. Trajectory optimization techniques are computationally expensive, especially when applied to nonlinear systems and long trajectories [5]. To reduce the computational cost, work has been done in learning a safe controller. However, learning-based controllers usually require unsafe interactions [1]. Recently, work has been done in ensuring safety also during learning [6] by switching between a safe backup and an exploration controller. However, this approach may generate jerky motions, making it less desirable for real-world applications.

CBFs provide a simple yet effective way to synthesize controllers for safety-critical applications [7]. The typical approach to finding a CBF is to start from the hard constraints and find a forward invariant function w.r.t. the safe set. This approach is viable for simple linear constraints. However, as the constraints’ complexity increases, especially when the

constraints are nonlinear or non-convex and when the system dynamics are nonlinear and have a high relative degree, it becomes increasingly difficult to find a suitable CBF by hand, e.g., dynamic walking on stepping stones [8] and Segway balancing [9]. However, finding an HCBF that only recovers a portion of the safe set is usually possible [10]. Instead of finding CBFs by hand, work has been done on learning CBFs using human demonstrations [3]. However, they require state trajectories along the safe set boundary, which is not always available. Work has also been done on learning CBFs from a safe and unsafe trajectories dataset [11]. Collecting a dataset of unsafe trajectories might be costly or even dangerous in many applications, e.g., autonomous driving. Instead of relying on external resources, CBF can also be synthesized online using onboard sensors [2]. This approach has the benefit of using only safe training data. However, it might not generalize outside object avoidance tasks well since not all safe set boundaries can be obtained through sensor measurements. In addition to finding a good CBF, work has been done on finding a looser CBF constraint under a given CBF [12]. However, this does not mitigate the issue of having conservative CBFs.

Another way to ensure safety is to incorporate the safety requirements as constraints of an optimization problem as in MPC [13]. MPC has been widely applied to autonomous driving [14] and bipedal locomotion [15], to name a few. More recently, work has been done in applying nonlinear MPC to quadrupedal systems [16]. However, compared to the solution time of a CBF-QP, solving MPC problems is usually time-consuming, which reduces applicability to real-time control. Thus, a multi-time scale control framework is typically used. MPC generates a reference trajectory at a lower frequency while a reactive controller runs at a high frequency to produce control signals sent to the system. Another issue with MPC is that the constraints only affect the control when the system is near the edge of the safe set. This can be alleviated by increasing the time horizon. However, the solution time would also be greatly increased.

In this paper, we propose an algorithmic approach to combine CBF and MPC-based approaches in learning a CBF that recovers a larger portion of the true safe set. The main contribution of this paper is twofold: (1) we develop a method to estimate the true CBF starting from an HCBF; (2) we show the effectiveness of the proposed method through simulation studies. The remainder of this paper is structured as follows. In Section II, the CBF and MPC approaches are briefly summarized. In Section III, the problem formulation for this paper is given. In Section IV, the proposed method is presented. In Section V, we show the efficacy of our approach

<sup>1</sup>Control/Robotics Research Laboratory, Electrical & Computer Engineering Department, Tandon School of Engineering, New York University, Brooklyn, NY, 11201 bd1555@nyu.edu, prashanth.krishnamurthy@nyu.edu, khorrami@nyu.edu

using simulation studies on three systems: 2D integrator, ball-on-beam, and unicycle. Finally, we conclude the paper with a summary and a discussion on future directions.

## II. PRELIMINARIES

### A. Control Barrier Function Based Safe Control

This section summarizes the approach of achieving certifiable safety critical control using CBFs. For a detailed review please refer to [17]. Consider a system in the control affine form

$$\dot{\mathbf{x}} = \mathbf{F}(\mathbf{x}) + \mathbf{G}(\mathbf{x})\mathbf{u} \quad (1)$$

with the states being denoted by  $\mathbf{x} \in \mathbb{R}^n$ , the control inputs by  $\mathbf{u} \in \mathbb{R}^m$ , the drift by  $\mathbf{F}(\mathbf{x}) : \mathbb{R}^n \rightarrow \mathbb{R}^n$ , and the control influence by  $\mathbf{G}(\mathbf{x}) : \mathbb{R}^n \rightarrow \mathbb{R}^{n \times m}$ . Additionally, we have a safe set  $\mathcal{C}$  defined as the superlevel set of a smooth function  $\mathbf{h}(\mathbf{x}) : \mathbb{R}^n \rightarrow \mathbb{R}$

$$\mathcal{C} = \{\mathbf{x} \mid \mathbf{h}(\mathbf{x}) \geq 0\}. \quad (2)$$

We can synthesize safe controllers by finding controls that satisfy the constraint

$$\frac{\partial \mathbf{h}(\mathbf{x})}{\partial \mathbf{x}} \dot{\mathbf{x}} \geq -\alpha(\mathbf{h}(\mathbf{x})) \quad (3)$$

where  $\alpha(\cdot)$  is a class  $\mathcal{K}_\infty$  function. There are two main frameworks for CBF-based safe control: (1) construct a quadratic program (QP) in combination with a control Lyapunov function (CLF), also known as CLF-CBF-QP; (2) construct a QP utilizing a performance controller  $\pi_{\text{perf}}(\mathbf{x}) : \mathbb{R}^n \rightarrow \mathbb{R}^m$ , also known as CBF-QP. The method we propose in this work is based on the latter formulation, thus, we give a brief introduction to CBF-QPs. The performance controller first provides a reference control action

$$\mathbf{u}_{\text{ref}} \sim \pi_{\text{perf}}(\mathbf{x}). \quad (4)$$

Note that this performance controller does not need to generate control actions that ensures the forward invariance of the safe set. We can then construct a QP

$$\min_{\mathbf{u}} \quad \|\mathbf{u}_{\text{ref}} - \mathbf{u}_{\text{safe}}\|^2 \quad (5)$$

$$\text{subject to} \quad L_{\mathbf{F}} \mathbf{h}(\mathbf{x}) + L_{\mathbf{G}} \mathbf{h}(\mathbf{x}) \mathbf{u}_{\text{safe}} \geq -\alpha(\mathbf{h}(\mathbf{x}))$$

which gives us the safe control action  $\mathbf{u}_{\text{safe}}$ , where  $L_{\mathbf{F}} \mathbf{h}(\mathbf{x})$  and  $L_{\mathbf{G}} \mathbf{h}(\mathbf{x})$  represents the Lie derivatives.

### B. Model Predictive Control

MPC is a widely used framework for solving finite-horizon optimal control problems. Define the instantaneous cost at time  $t$  as  $\ell(\mathbf{x}(t), \mathbf{u}(t), t)$ . The MPC objective is to minimize the sum of the instantaneous costs over a predefined time horizon  $T$  subject to constraints, which can be written as

$$\min_{\mathbf{u}} \quad \int_{t_0}^{t_0+T} \ell(\mathbf{x}(t), \mathbf{u}(t), t) dt \quad (6)$$

$$\text{subject to} \quad \dot{\mathbf{x}}(t) = \mathbf{F}(\mathbf{x}(t)) + \mathbf{G}(\mathbf{x}(t))\mathbf{u}(t) \\ \mathbf{c}(\mathbf{x}(t)) \leq \mathbf{b}.$$

with  $\mathbf{c} : \mathbb{R}^n \rightarrow \mathbb{R}^r$  being a vector of functions of the state and  $\mathbf{b} \in \mathbb{R}^r$  representing the element-wise upper bound of  $\mathbf{c}(\cdot)$ . Note that control saturation can also be incorporated, but it is not included in (6) for brevity. The solution to the MPC problem gives the optimal control actions over the time interval  $[t_0, t_0+T]$ . MPC provides a robust framework for generating control actions by iterating this process. One major drawback for MPC is that with the increase in horizon length, the solution time would also grow, making it difficult to deploy directly to real-time control tasks.

## III. PROBLEM FORMULATION

In this work, we consider systems in the form of (1). We have the following assumptions:

- 1) we have access to a performance controller  $\pi_{\text{perf}}(\mathbf{x})$  that enables the system (1) to achieve a certain task, e.g., target reaching;
- 2) we have access to an accurate estimation of the true system dynamics (this is a commonly used assumption in previous works on CBFs [11] [12]);
- 3) the safe set  $\mathcal{C}$  is defined as the largest set in  $\{\mathbf{x} \mid \mathbf{c}(\mathbf{x}) \leq \mathbf{b}\}$  where  $\exists \mathbf{u}$  that renders it forward invariant;
- 4) we do not have access to an accurate CBF.

We define the CBF that recovers the safe set  $\mathcal{C}$  as  $\mathbf{h}(\mathbf{x})$ , which satisfies

$$\mathcal{C} = \{\mathbf{x} \mid \mathbf{h}(\mathbf{x}) \geq 0\}. \quad (7)$$

Utilizing  $\mathbf{h}(\mathbf{x})$ , we can formulate a CBF-QP that gives us the safe control action  $\mathbf{u}_{\text{safe}}$ .

However, in general, it is difficult to find a CBF that recovers the true safe set  $\mathcal{C}$  [10]. But it is usually viable to find a CBF  $\hat{\mathbf{h}}(\mathbf{x})$  such that the safe set it defines is a subset of the true safe set, i.e.,

$$\hat{\mathcal{C}} = \{\mathbf{x} \mid \hat{\mathbf{h}}(\mathbf{x}) \geq 0\} \subseteq \mathcal{C}. \quad (8)$$

We refer to such a CBF  $\hat{\mathbf{h}}$  that we can find analytically as a "handcrafted" CBF. As discussed above, handcrafted CBFs are often conservative in practice since they provide an underestimate of the true safe region. Without loss of generality, we can assume the relationship

$$\mathbf{h}(\mathbf{x}) = \hat{\mathbf{h}}(\mathbf{x}) + \Delta \mathbf{h}(\mathbf{x}). \quad (9)$$

In this work, we aim to find an algorithmic approach to generate a good estimate of  $\Delta \mathbf{h}(\mathbf{x})$ . Defining the safe set recovered by the estimated CBF as

$$\tilde{\mathcal{C}} = \{\mathbf{x} \mid \hat{\mathbf{h}}(\mathbf{x}) + \Delta \hat{\mathbf{h}}(\mathbf{x}) \geq 0\}, \quad (10)$$

where  $\Delta \hat{\mathbf{h}}(\mathbf{x})$  is an estimation of  $\Delta \mathbf{h}(\mathbf{x})$ . The following relationship should hold

$$\hat{\mathcal{C}} \subseteq \tilde{\mathcal{C}} \approx \mathcal{C}. \quad (11)$$

In situations where recovering the true safe set is not relevant to achieving the given task, the expanded safe set  $\tilde{\mathcal{C}}$  should ensure the task is better achieved, e.g., having lower cost.

## IV. METHOD

In this section, we detail our proposed approach of learning an estimate of the true CBF starting from an HCBF. We separate the discussion into two sections: loss function design and data collection.

### A. Loss Function Design

In this section, we will discuss the loss functions design for learning  $\tilde{\mathbf{h}}(\mathbf{x})$  such that

$$\tilde{\mathbf{h}}(\mathbf{x}) = \hat{\mathbf{h}}(\mathbf{x}) + \Delta\hat{\mathbf{h}}(\mathbf{x}) \quad (12)$$

is a good estimation of the true CBF  $\mathbf{h}(\mathbf{x})$ . The conditions a valid CBF should satisfy are

$$\tilde{\mathbf{h}}(\mathbf{x}) > 0 \quad \forall \mathbf{x} \in \text{Int } \mathcal{C} \quad (13a)$$

$$\tilde{\mathbf{h}}(\mathbf{x}) < 0 \quad \forall \mathbf{x} \in \setminus \mathcal{C}. \quad (13b)$$

In addition to these two conditions, to obtain safe control actions, the partial derivative of  $\tilde{\mathbf{h}}(\mathbf{x})$  w.r.t. the state should also satisfy

$$L_{\mathbf{F}}\tilde{\mathbf{h}}(\mathbf{x}) + L_{\mathbf{G}}\tilde{\mathbf{h}}(\mathbf{x})\mathbf{u} + \alpha(\tilde{\mathbf{h}}(\mathbf{x})) \geq 0 \quad \forall \mathbf{x} \in \mathcal{C} \quad (14)$$

with  $\mathbf{u}$  being a safe action.

Although (13a) is the sole requirement for CBF values within the safe set; we can add additional constraints to the CBF value to guide the learning process better. We force the CBF value for states within the safe set to increase with their distance from the constraint boundary. Note that the CBF values for states on the constraint boundary should be less than or equal to zero. Using these two constraints, we change the condition in (13a) into

$$\hat{\mathbf{h}}(\mathbf{x}_i) + \Delta\hat{\mathbf{h}}(\mathbf{x}_i) \geq \mathbf{d}_+(\mathbf{x}_i) \quad \forall \mathbf{x} \in \mathcal{C} \quad (15)$$

with  $\mathbf{d}_+(\mathbf{x}) \in \mathbb{R}_+$  being a function computing the distance between the current state and the constraint boundary. For examples regarding the choice of  $\mathbf{d}_+(\mathbf{x})$  please refer to Section V. To encourage the relationship in (15), we construct the loss function

$$\mathcal{L}_{\mathbf{h}} = \frac{1}{N_{\text{safe}}} \sum_{i=1}^{N_{\text{safe}}} \max \left( 0, -\hat{\mathbf{h}}(\mathbf{x}_i) - \Delta\hat{\mathbf{h}}(\mathbf{x}_i) + \mathbf{d}_+(\mathbf{x}_i) \right). \quad (16)$$

where  $N_{\text{safe}}$  is the size of safe dataset. It can be seen that  $\mathcal{L}_{\mathbf{h}}$  is minimized when (15) is satisfied for all of the data points  $\mathbf{x}_i$ .

Like safe interactions, even though (13b) is the only condition required for a valid CBF, the learning process would greatly benefit from stronger conditions. We force the CBF value for unsafe data points to decrease as it moves further into the interior of the unsafe set. Using another function  $\mathbf{d}_-(\mathbf{x}) \in \mathbb{R}_-$ , we can write the condition unsafe data points should satisfy as

$$\hat{\mathbf{h}}(\mathbf{x}_i) + \Delta\hat{\mathbf{h}}(\mathbf{x}_i) \leq \mathbf{d}_-(\mathbf{x}) \quad \forall \mathbf{x} \in \setminus \mathcal{C} \quad (17)$$

Rewriting the condition in (17) into a loss function, we have

$$\mathcal{L}_{\mathbf{d}} = \frac{1}{N_d} \sum_{i=1}^{N_d} \max \left( 0, \hat{\mathbf{h}}(\mathbf{x}_i^d) + \Delta\hat{\mathbf{h}}(\mathbf{x}_i^d) - \mathbf{d}_-(\mathbf{x}_i^d) \right). \quad (18)$$

where  $N_d$  is the size of unsafe dataset. The superscript ‘d’ represents that the states are sampled from the unsafe (dangerous) dataset.

To be able to synthesize safe control actions using the learned CBF, we would also require it to satisfy the CBF constraints (14). Using the same logic in constructing (16), we can write a loss function that is minimized when (14) is satisfied for all data points

$$\begin{aligned} \mathcal{L}_{\nabla \mathbf{h}} = \frac{1}{N_{\text{safe}}} \sum_{i=1}^{N_{\text{safe}}} & \max \left( 0, \right. \\ & \left. - L_{\mathbf{F}}\tilde{\mathbf{h}}(\mathbf{x}_i) - L_{\mathbf{G}}\tilde{\mathbf{h}}(\mathbf{x}_i)\mathbf{u}_i - \alpha(\tilde{\mathbf{h}}(\mathbf{x}_i)) \right). \end{aligned} \quad (19)$$

Unique to our problem is that there are much more safe data compared to unsafe data (the generation of unsafe data will be discussed in Section IV-B). Thus, we need to ensure that the learned CBF does not simply output a positive value for any  $\mathbf{x}$ . We achieve this by regulating the change introduced by  $\Delta\hat{\mathbf{h}}(\mathbf{x})$ . The logic behind this choice is that for unsafe states, the HCBF  $\hat{\mathbf{h}}(\mathbf{x})$  already gives them a negative value. By regulating the change introduced by  $\Delta\hat{\mathbf{h}}(\mathbf{x} | \theta)$  we aim to only make the CBF values for the safe states positive while keeping the unsafe states negative. To achieve this, we construct the loss function

$$\mathcal{L}_{\Delta\mathbf{h}} = \frac{1}{N_{\text{safe}}} \sum_{i=1}^{N_{\text{safe}}} \Delta\hat{\mathbf{h}}^2(\mathbf{x}_i) \quad (20)$$

We then have the final loss function as

$$\mathcal{L} = \mathcal{L}_{\mathbf{h}} + \lambda_1 \mathcal{L}_{\mathbf{d}} + \mathcal{L}_{\nabla \mathbf{h}} + \lambda_2 \mathcal{L}_{\Delta\mathbf{h}} \quad (21)$$

where  $\lambda_1, \lambda_2 \in \mathbb{R}_+$  weights the importance of  $\mathcal{L}_{\mathbf{d}}$  and  $\mathcal{L}_{\Delta\mathbf{h}}$ , respectively. Since estimating part of the unsafe set as safe is much more disastrous than estimating part of the safe set as unsafe,  $\lambda_1$ , if not zero, is usually set to be larger than one. The choice of  $\lambda_2$  is task dependent. Some example settings can be seen in Section V.

To learn  $\Delta\hat{\mathbf{h}}(\mathbf{x})$  using the loss in (21), We use a neural network to represent  $\Delta\hat{\mathbf{h}}(\mathbf{x})$  which is parameterized by  $\theta$ . The learned CBF is denoted as

$$\tilde{\mathbf{h}}(\mathbf{x} | \theta) = \hat{\mathbf{h}}(\mathbf{x}) + \Delta\hat{\mathbf{h}}(\mathbf{x} | \theta). \quad (22)$$

We represent the safe and unsafe dataset as

$$\mathcal{X} = \{\mathbf{x}_i\}_{i=1}^N, \quad \mathcal{X}_{\mathbf{d}} = \{\mathbf{x}_i^d\}_{i=1}^M. \quad (23)$$

where  $\mathcal{X}$  is the safe dataset and  $\mathcal{X}_{\mathbf{d}}$  is the unsafe data set, the subscript  $\mathbf{d}$  denotes dangerous. The collection process of the two dataset will be described in Section IV-B.

### B. Data Collection

As mentioned in Section IV-A, learning  $\tilde{\mathbf{h}}(\mathbf{x} | \theta)$  requires both safe and unsafe data. However, the collection of unsafe data may be costly in many cases, e.g., autonomous driving. Instead of finding an unsafe controller, we can perform model-based rollouts to generate ‘fake’ data. During training, we use a CBF-QP controller with the learned CBF  $\tilde{\mathbf{h}}(\mathbf{x}) + \Delta\hat{\mathbf{h}}(\mathbf{x} | \theta)$  to collect safe interactions. Note that unless

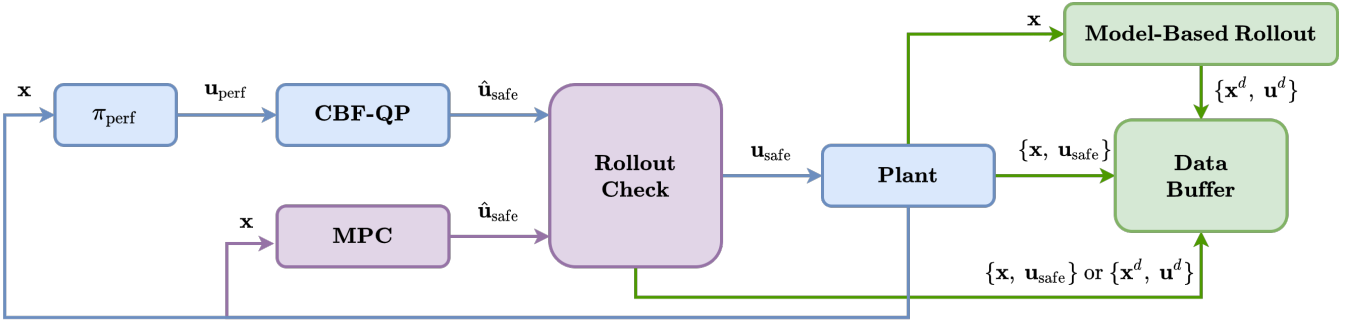


Fig. 1. This figure illustrates the data collection process. The blue arrows represents the control loop that is performed at each timestep. The purple arrows represents the control loop that is performed every  $r_{CBFQP}$  timesteps. The green arrows represents storing the collected data.

### Algorithm 1 Algorithm for Learning a Better CBF

```

1: Given:
2:  $\mathbf{F}(\mathbf{x}), \mathbf{G}(\mathbf{x})$ : state dynamics;
3:  $\hat{\mathbf{h}}(\mathbf{x})$ : handcrafted CBF,  $\alpha(\cdot)$ : class  $\mathcal{K}_\infty$  function;
4:  $\pi_{\text{perf}}, \pi_{\text{MPC}}$ : performance controller and MPC controller;
5:  $N$ : Episode length,  $L$ : Number of iterations,  $M$ : Batch size;
6:  $\theta_1$ : initialized neural network weights;
7:  $\lambda_1, \lambda_2$ : loss weights;
8: for  $l = 1$  to  $L$  do
9:   for  $n = 1$  to  $N$  do
10:     $\mathbf{u}_{\text{ref}} = \pi_{\text{perf}}(\mathbf{x}_n)$ ;
11:    Run CBF-QP using  $\hat{\mathbf{h}}(\mathbf{x}) + \Delta\hat{\mathbf{h}}(\mathbf{x} \mid \theta_l)$  and get
         $\mathbf{u}_{\text{safe}}$ ;
12:    if  $n \% r_{CBFQP} = 0$  then
13:      Perform model-based rollout using CBF-QP
14:      if unsafe state encountered then
15:         $\mathbf{u}_{\text{safe}} = \pi_{\text{MPC}}(\mathbf{x})$ 
16:        Store safe data in  $\mathcal{X}$ 
17:        Store unsafe data in  $\mathcal{X}^d$ 
18:      if  $\mathbf{c}(\mathbf{x}) - \mathbf{b} \geq -\epsilon_c$  then
19:        Perform model-based rollout using  $\pi_{\text{perf}}$ 
20:        Store safe data in  $\mathcal{X}$ 
21:        Store unsafe data in  $\mathcal{X}^d$ 
22:      Step the environment and store  $\{\mathbf{x}_n, \mathbf{u}_{\text{safe}}\}$ ;
23:      Update  $\theta_l$  using  $\mathcal{L}$  and obtain  $\theta_{l+1}$ ;
24: End algorithm;

```

$\Delta\hat{\mathbf{h}}(\mathbf{x} \mid \theta)$  is fully trained, there is no guarantee that the learned CBF corresponds to a safe set. To deal with this issue, the controller performs a rollout using the CBF-QP controller every  $r_{CBFQP}$  steps. If the rollout generates unsafe data, the data is recorded, and an MPC controller is invoked to generate safe control actions. Using this approach, we can obtain both safe and unsafe data while not endangering the system.

In addition to the model-based rollout mentioned above, model-based rollout can also be performed when the system is close to the constraint boundary. To check whether the

current state is close to the constraint boundary, we define  $\epsilon_c \in \mathbb{R}_+$ , and whenever

$$\mathbf{c}(\mathbf{x}) - \mathbf{b} \geq -\epsilon_c \quad (24)$$

a model-based rollout can be performed. The value of  $\epsilon_c$  is task-dependent and is a hyperparameter that needs to be tuned. When performing the rollout, the performance controller  $\pi_{\text{perf}}$  is used to generate control actions, which is generally an unsafe controller. In our experiments, we either only use the CBF-QP-based rollouts or both. A diagram of the data collection process is given in Figure 1. A detailed description of the learning and data collection process can be found in Alg. 1.

## V. SIMULATION

In this section, we demonstrate our proposed approach on three tasks. The first task, 2D integrator target reaching with velocity constraint, is a toy example where the learned CBF can be plotted and analyzed. The second task, ball-on-beam balancing with angle constraint, demonstrates our approach on a nonlinear system. It also shows the robustness of our proposed method by showing the CBF constraint can be altered after training to produce controllers with varying aggressiveness when approaching the constraint boundary. For the third task, unicycle target reaching with obstacle avoidance, we further test the robustness of our method by showing that the performance controller can be arbitrarily switched. All of the training is performed using PyTorch.

### A. Deep Differential Network

When utilizing the learned CBF in the simulation studies, a CBF-QP (5) is solved to find the safe control. Therefore we need to compute  $\partial\Delta\hat{\mathbf{h}}(\mathbf{x} \mid \theta)/\partial\mathbf{x}$ . Instead of using numerical methods, e.g., automatic differentiation, we find its value analytically using deep differential networks [18]. At each layer, the partial derivative of the output  $\mathbf{y}' \in \mathbb{R}^{n_o \times 1}$  w.r.t. the input  $\mathbf{y} \in \mathbb{R}^{n_i \times 1}$  is computed as

$$\frac{\partial \mathbf{y}'}{\partial \mathbf{y}} = \text{diag}(\mathbf{g}'(\mathbf{a})) \mathbf{W} \quad (25)$$

where  $\mathbf{W} \in \mathbb{R}^{n_o \times n_i}$  represents the weights of that layer,  $\mathbf{g} : \mathbb{R}^{n_o \times 1} \rightarrow \mathbb{R}^{n_o \times 1}$  represents the activation function,  $\mathbf{g}'(\cdot)$

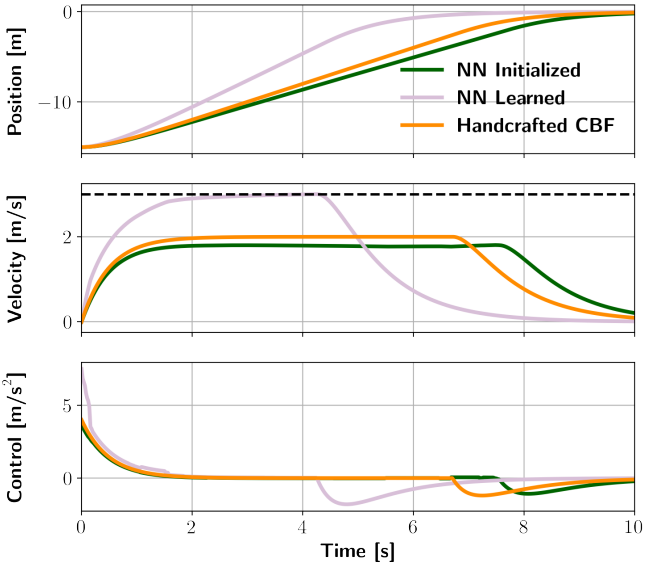


Fig. 2. This figure shows the state and control trajectories of the CBF-QP controller using different CBFs. The NN Initialized trajectory is obtained using the CBF  $\hat{\mathbf{h}}(\mathbf{x}) + \Delta\hat{\mathbf{h}}(\mathbf{x} | \theta_1)$ , the NN Learned is obtained using the CBF  $\hat{\mathbf{h}}(\mathbf{x}) + \Delta\hat{\mathbf{h}}(\mathbf{x} | \theta_N)$ , and the Handcrafted CBF trajectory is obtained using the CBF  $\hat{\mathbf{h}}(\mathbf{x})$ . The dashed line in the velocity plot corresponds to  $\dot{x} = 3$  which represents the velocity constraint.

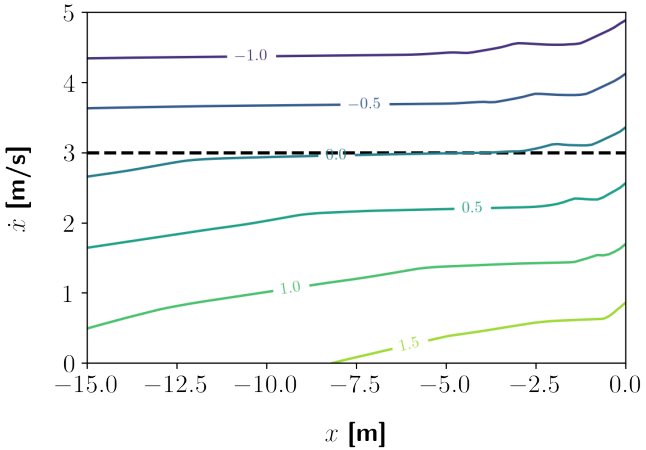


Fig. 3. This figure shows the contour of the learned CBF. The black dashed line denotes the zero level line of the true CBF, the region above the dashed line will be negative for the true CBF and positive below.

represents the derivative of the activation function, and  $\mathbf{a} = \mathbf{W}\mathbf{y} + \text{bias}$ . In all our experiments, we use a network of three layers. The output size of each layer is  $[128, 128, 1]$ . All of the activation functions are Softplus.

### B. 2D Integrator Target Reaching + Velocity Constraint

The 2D integrator has the system dynamics of

$$\begin{bmatrix} \dot{x} \\ \ddot{x} \end{bmatrix} = \begin{bmatrix} 0 & 1 \\ 0 & 0 \end{bmatrix} \begin{bmatrix} x \\ \dot{x} \end{bmatrix} + \begin{bmatrix} 0 \\ 1 \end{bmatrix} \mathbf{u} \quad (26)$$

with  $x$  denoting the position and  $\dot{x}$  denoting the velocity. The dynamics (26) can also be written as

$$\dot{\mathbf{x}} = \mathbf{A}\mathbf{x} + \mathbf{B}\mathbf{u}. \quad (27)$$

with  $\mathbf{x} \in \mathbb{R}^2$ ,  $\mathbf{A} \in \mathbb{R}^{2 \times 2}$ ,  $\mathbf{B} \in \mathbb{R}^{2 \times 1}$ , and  $\mathbf{u} \in \mathbb{R}$ . The velocity constraint has the form of

$$\dot{x} \leq 3.0. \quad (28)$$

We construct an HCBF

$$\hat{\mathbf{h}}(\mathbf{x}) = 2 - \dot{x} \quad (29)$$

which corresponds to the velocity constraint

$$\dot{x} \leq 2.0. \quad (30)$$

The task is to start from  $[\mathbf{x}_{\text{init}}, 0]$  and reach the origin. The performance controller is a LQR controller with the weights

$$\mathbf{Q} = \begin{bmatrix} 10 & 0 \\ 0 & 10 \end{bmatrix} \quad \mathbf{R} = [1]. \quad (31)$$

The MPC formulation is

$$\min_{\mathbf{u}_i \text{'s}} \sum_{i=1}^T \frac{1}{2} \mathbf{x}_i^T \mathbf{Q} \mathbf{x}_i + \frac{1}{2} \mathbf{u}_i^T \mathbf{R} \mathbf{u}_i \quad (32)$$

subject to  $\mathbf{x}_0 = \mathbf{x}$

$$\dot{\mathbf{x}}_i = \mathbf{A}\mathbf{x}_i + \mathbf{B}\mathbf{u}_i$$

$$\dot{x}_i \leq 3.0.$$

We set  $\lambda_1 = 0$  and  $\lambda_2 = 1$ . The CBF is trained for 100 epochs with a learning rate of  $10^{-3}$ . During training, the initial state  $\mathbf{x}_{\text{init}}$  for each episode is randomly sampled from  $[-15, -5]$ . We set

$$\mathbf{d}_+(\mathbf{x}) = \mathbf{d}_-(\mathbf{x}) = 3 - \dot{x}. \quad (33)$$

We pick the class  $\mathcal{K}_\infty$  function

$$\alpha(\mathbf{h}(\mathbf{x})) = \gamma \mathbf{h}(\mathbf{x}) \quad (34)$$

for the CBF-QP constraint (14). Since this is a toy example, we can also construct a CBF for the true constraint (28)

$$\mathbf{h}(\mathbf{x}) = 3 - \dot{x} \quad (35)$$

and compare it with the learned CBF. Under the aforementioned setting, using Algorithm 1, the state trajectory when using the learned CBF in a CBF-QP controller is shown in Figure 2, with  $\mathbf{x}_{\text{init}} = -15$ . During training, both CBF-QP-based rollouts and model-based rollouts are performed. The contour plot of the learned CBF is shown in Figure 3.

From Figure 2, we can see that the learned CBF can recover the original velocity constraint (28) since the velocity saturates at 3m/s. The handcrafted CBF curve underestimates the velocity constraints, while the NN initialized curve is dependent on the initialization of the neural network weights. From Figure 3, we can see that the zero level set of the learned CBF is almost the same as the zero level set of the true CBF. There are inaccuracies in estimating where the zero level line should be when  $x$  is close to  $-15$  and  $0$ . This is due to having no data with  $\dot{x}$  close to 3m/s at the beginning and at the end of the trajectory. This example shows that our proposed approach can learn a better estimate of the true CBF starting from a conservative estimation.

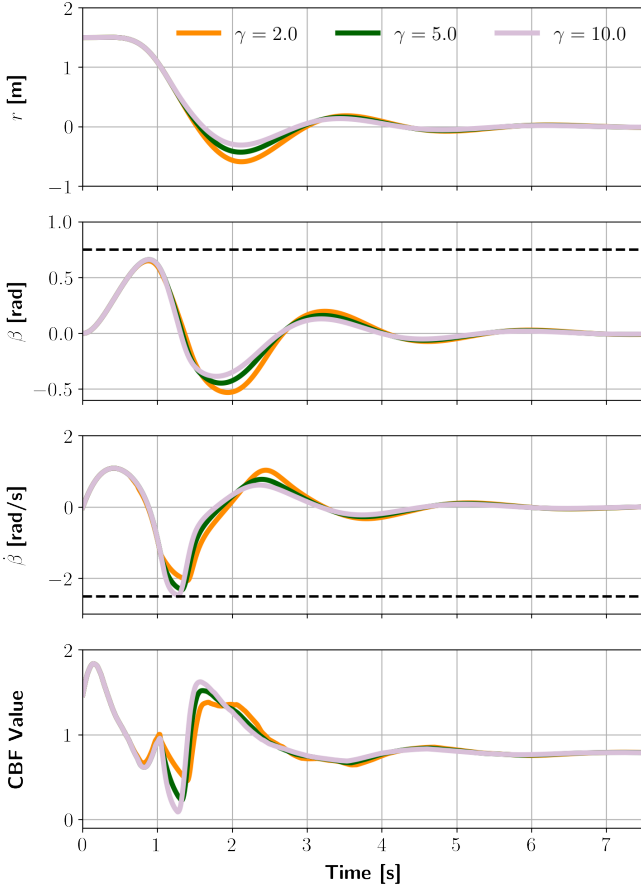


Fig. 4. This figure illustrates the motion and CBF values under the learned CBF controller for the ball-on-beam simulations. The upper three plots illustrates the motion generated by the learned CBF under different values of  $\alpha(\mathbf{h}(\mathbf{x})) = \gamma \mathbf{h}(\mathbf{x})$  in the CBF-QP constraint. The dashed black line plots represents the constraints  $\beta \leq 0.75$  and  $\dot{\beta} \geq -2.5$ . The lowest plot illustrates the CBF values along the trajectories.

### C. Ball-on-beam Balancing + Angle & Angular Velocity Constraint

The ball-on-beam system has the dynamics

$$\begin{bmatrix} \dot{r} \\ \dot{\beta} \\ \ddot{r} \\ \ddot{\beta} \end{bmatrix} = \begin{bmatrix} \dot{r} \\ \dot{\beta} \\ \frac{5}{7}(r\dot{\beta}^2 - g \sin \beta) \\ -\frac{2mr\dot{r}\dot{\beta} + mgr \cos \beta}{I_{\text{beam}} + mr^2} \end{bmatrix} + \begin{bmatrix} 0 \\ 0 \\ 0 \\ 1 \end{bmatrix} \tau \quad (36)$$

with  $r$  being the position of the ball along the beam,  $\beta$  being the angle of the beam,  $m$  is the mass of the ball,  $g$  is the gravitational acceleration,  $I_{\text{beam}}$  is the moment of inertia of the beam, and  $\tau$  is a torque applied to the beam. The equations in (36) can be written as

$$\dot{\mathbf{x}} = \mathbf{F}(\mathbf{x}) + \mathbf{G}(\mathbf{x})\mathbf{u} \quad (37)$$

with  $\mathbf{x} \in \mathbb{R}^4$ ,  $\mathbf{F} : \mathbb{R}^4 \rightarrow \mathbb{R}^{4 \times 1}$ ,  $\mathbf{G} : \mathbb{R}^4 \rightarrow \mathbb{R}^{4 \times 1}$ , and  $\mathbf{u} \in \mathbb{R}$ . We want to find a single CBF corresponding to the beam

angle and angular velocity constraints

$$\beta \leq 0.75 \quad (38a)$$

$$\dot{\beta} \geq -2.5. \quad (38b)$$

However, we find that it is difficult to construct even a conservative HCBF that is able to combine these two constraints. Instead, we start from the HCBF

$$\hat{\mathbf{h}}(\mathbf{x}) = -\dot{\beta} + \gamma_0(\bar{\beta} - \beta) \quad (39)$$

which corresponds to the beam angle constraint

$$\beta \leq \bar{\beta}. \quad (40)$$

We pick  $\bar{\beta} = 0.5$  so that the motion generated under the HCBF would also not violate the angular velocity constraint. Starting from (39), we learn a CBF that is able to recover the safe set described by (38). The objective is to move the ball from  $r = r_{\text{init}}$  to  $r = 0$ . The initial state is  $[r_{\text{init}}, 0, 0, 0]^T$ , the target state is  $[0, 0, 0, 0]^T$ . The performance controller is a LQR controller using the linearized dynamics with the cost matrices as

$$\mathbf{Q} = \begin{bmatrix} 10 & 0 & 0 & 0 \\ 0 & 1 & 0 & 0 \\ 0 & 0 & 1 & 0 \\ 0 & 0 & 0 & 1 \end{bmatrix} \quad \mathbf{R} = [1]. \quad (41)$$

For the MPC controller, we use the nonlinear MPC (NMPC) package `do-mpc` [19]. The NMPC problem has the form of

$$\min_{\mathbf{u}_i \text{'s}} \sum_{i=1}^T \frac{1}{2} \mathbf{x}_i^T \mathbf{Q} \mathbf{x}_i + \frac{1}{2} \mathbf{u}_i^T \mathbf{R} \mathbf{u}_i \quad (42)$$

subject to  $\mathbf{x}_0 = \mathbf{x}$

$$\dot{\mathbf{x}}_i = \mathbf{F}(\mathbf{x}_i) + \mathbf{G}(\mathbf{x}_i)\mathbf{u}_i$$

$$\beta \leq 0.75$$

$$\dot{\beta} \geq -2.5.$$

We set  $\lambda_1 = 2$ ,  $\lambda_2 = 0$ . The class  $\mathcal{K}_\infty$  function  $\alpha(\cdot)$  is picked as in (34), with  $\gamma = 2.0$  during training. The distance functions are chosen to be

$$\mathbf{d}_+(\mathbf{x}) = \min(0.75 - \beta, \dot{\beta} + 2.5) \quad (43a)$$

$$\mathbf{d}_-(\mathbf{x}) = \max(0.75 - \beta, \dot{\beta} + 2.5). \quad (43b)$$

The CBF is trained for 1000 epochs with a learning rate of  $10^{-4}$ . During training only CBF-QP-based rollouts are performed. The motion generated using the learned CBF is shown in Figure 4. To show the robustness of the learned CBF, we tested the learned CBF using different values of  $\gamma$ , the generated motion can also be seen in Figure 4. The trajectories generated by different  $\gamma$  values are all safe trajectories. The learned CBF values along the trajectories are shown in Figure 4. It can be seen that as  $\gamma$  increases, the smallest CBF value along the trajectory gets closer to zero, which aligns with the role  $\gamma$  plays in CBF-QPs. This example shows that our proposed approach can be applied to nonlinear systems and the learned CBF is robust such that the CBF constraint can be tweaked after training.

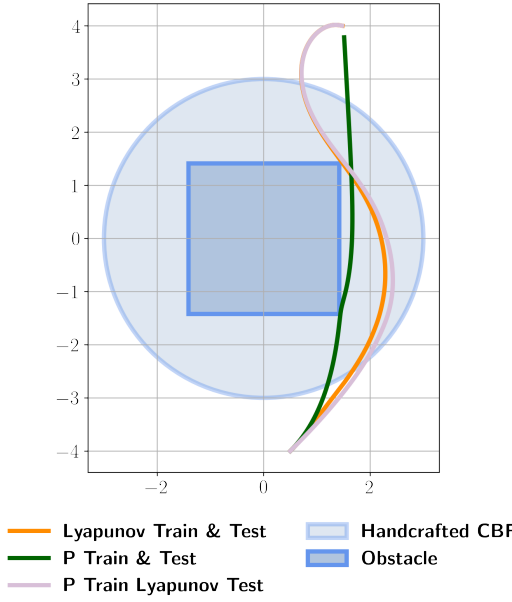


Fig. 5. This figure shows the motion generated under different training and testing configurations. The “Lyapunov Train & Test” represents the same Lyapunov-based controller is used for data collection during training and also testing. “P Train & Test” denotes the proportional controller in (54) is used for both training and testing. The “P Train Lyapunov Test” represents the data used for learning the CBF is collected using the proportional controller while the testing is done using the Lyapunov-based controller. The square block corresponds to the true obstacle. The larger circle represents the unsafe region corresponding to the HCBF.

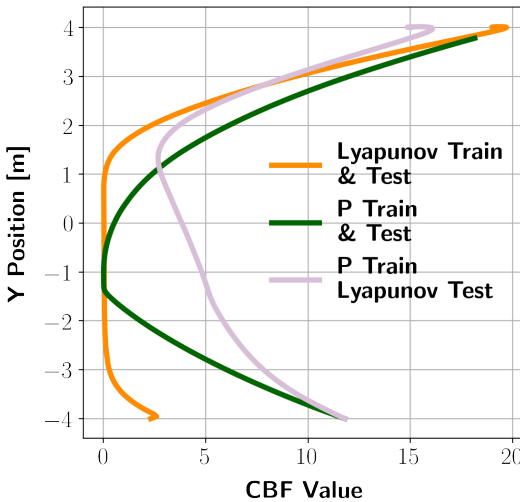


Fig. 6. This figure shows the CBF value evolution along the trajectory and its corresponding position along the Y axis.

#### D. Unicycle Target Reaching + Obstacle Avoidance

In previous simulation studies, a true CBF that recovers the safe set can be obtained. In this section, we test our proposed method to learn a CBF in a scenario in which it is very difficult (if not practically infeasible) to write an accurate

CBF by hand. The unicycle system has the dynamics

$$\begin{bmatrix} \dot{x} \\ \dot{y} \\ \dot{\phi} \end{bmatrix} = \begin{bmatrix} \cos \phi & 0 \\ \sin \phi & 0 \\ 0 & 1 \end{bmatrix} \begin{bmatrix} v \\ \omega \end{bmatrix} \quad (44)$$

with  $x$  denoting the position of the unicycle along the  $x$  axis,  $y$  denoting the position along the  $y$  axis, and  $\phi$  denoting the heading of the unicycle. The dynamics (44) can also be written as

$$\dot{\mathbf{x}} = \mathbf{G}(\mathbf{x})\mathbf{u}. \quad (45)$$

with  $\mathbf{G} : \mathbb{R}^3 \rightarrow \mathbb{R}^{3 \times 2}$ . The obstacle has the shape of a square. When constructing a CBF for a square obstacle, it is very difficult to analytically write a CBF that models the combination of exact constraints on the  $X$  and  $Y$  axes – instead, approximating the square by a circle makes it easier to construct an HCBF. The square obstacle has size  $2 \times 2$  and is centered at the origin. We approximate the square obstacle using a circle that corresponds to the non-convex constraint

$$x^2 + y^2 \geq 3^2. \quad (46)$$

The radius of the circle is chosen such that it is slightly larger than the square obstacle to account for measurement errors of the square in a more realistic setting. This would give us a conservative estimation of the unsafe region. The HCBF design is inspired by the CBF constructed in [20]

$$\hat{\mathbf{h}}(\mathbf{x}) = x^2 + y^2 + 2xl \cos \phi + 2yl \sin \phi + l^2 - r^2 \quad (47)$$

where  $r$  is the radius of the circle and  $l$  is a lookahead distance. For the performance controller, we use a Lyapunov-based controller. The Lyapunov function [21] is chosen to be

$$\mathbf{V}(\mathbf{x}) = \frac{1}{2}\lambda e^2 + \frac{1}{2}(\alpha^2 + h\beta^2) \quad (48)$$

with  $\lambda, h \in \mathbb{R}_+$  and

$$\begin{cases} e = \sqrt{(x - x^*)^2 + (y - y^*)^2} \\ \beta = \text{atan2}(y^* - y, x^* - x) \\ \alpha = \beta - \phi \end{cases} \quad (49)$$

where  $(x^*, y^*)$  represents the target position. The NMPC problem has the form of

$$\min_{\mathbf{u}_i \text{'s}} \sum_{i=1}^T \frac{1}{2}(\mathbf{x}_i - \mathbf{x}^*)^T \mathbf{Q}(\mathbf{x}_i - \mathbf{x}^*) + \frac{1}{2}\mathbf{u}_i^T \mathbf{R}\mathbf{u}_i \quad (50)$$

subject to  $\mathbf{x}_0 = \mathbf{x}$

$$\dot{\mathbf{x}}_i = \mathbf{G}(\mathbf{x}_i)\mathbf{u}_i$$

$$\mathbf{c}(\mathbf{x}_i) \leq \mathbf{b}$$

with

$$\mathbf{Q} = \begin{bmatrix} 10 & 0 & 0 \\ 0 & 10 & 0 \\ 0 & 0 & 1 \end{bmatrix} \quad \mathbf{R} = \begin{bmatrix} 1 & 0 \\ 0 & 1 \end{bmatrix}. \quad (51)$$

The value of  $\mathbf{c}(\cdot)$  and  $\mathbf{b}$  depends on where you are in the state space – i.e., whether you are closer to the obstacle on the  $X$  or the  $Y$  axis, e.g., if  $\mathbf{x}_0 = (0, -3)$  then

$$\mathbf{c}(\mathbf{x}_i) = y_i \quad \mathbf{b} = -\frac{\ell}{2}. \quad (52)$$

with  $\ell$  being the width of the square. We set  $\lambda_1 = 100$ ,  $\lambda_2 = 0$ . The CBF is trained for 1000 epochs with a learning rate of  $10^{-4}$ . We pick the class  $\mathcal{K}_\infty$  function as in (34) and

$$\mathbf{d}_+(\mathbf{x}) = \mathbf{d}_-(\mathbf{x}) = \max(|x|, |y|) - \ell/2. \quad (53)$$

During training, we set  $\gamma = 10.0$  and only CBF-QP-based rollouts are performed. Following Alg. 1, the motion generated using the learned CBF in a CBF-QP framework is shown in Figure 5 (“Lyapunov Train & Test”). To further validate the robustness of our approach, we test the learned CBF-QP performance when different performance controllers are used training and testing. For this purpose, we train the CBF using data collected with a CBF-QP under the performance controller

$$v = k_v e \quad (54a)$$

$$\omega = k_\omega(\beta - \phi) \quad (54b)$$

and test it using the Lyapunov-based controller, the motion is also shown in Figure 5 (“P Train Lyapunov Test”). We compare its motion with the “Lyapunov Train & Test” and the “P Train & Test” controllers. It can be seen that the testing motion for the two Lyapunov controllers are very similar even though the CBF is learned with different controllers during training. However, the motion of the “P Train & Test” controller is very different from the other two. This is not due to the learned CBF but how the P controller is designed. The P controller is designed to reach the target while disregarding its orientation, while the Lyapunov function tries to correct the heading as it approaches the target. The CBF value along the three trajectories are shown in Fig. 6. It can be seen that the CBF value is dependent on the training controller. When combining the information in Fig. 5 and Fig. 6, we see that under different settings, our proposed method learns different CBFs. However, the learned CBF all generates safe motions and learns a relatively good estimation of the true safe set.

## VI. CONCLUSION

In this paper, we proposed a learning-based approach to estimate the CBF that recovers the true safe set starting from a conservative HCBF. We designed an algorithmic data collection procedure that ensures safety. Additionally, unsafe data are generated synthetically during training using model-based rollouts. We tested our proposed approach on three different systems and tasks. Potential future directions include application to more complex systems and incorporation of inaccurate or learned dynamics.

## REFERENCES

- [1] B. Dai, P. Krishnamurthy, A. Papanicolaou, and F. Khorrami, “State constrained stochastic optimal control using LSTMs,” in *Proceedings of American Control Conference, ACC, New Orleans, LA, May 25-28, 2021*, pp. 1294–1299.
- [2] M. Srinivasan, A. Dabholkar, S. Coogan, and P. A. Vela, “Synthesis of control barrier functions using a supervised machine learning approach,” in *Proceedings of IEEE/RSJ International Conference on Intelligent Robots and Systems, IROS, Las Vegas, NV, October 24, 2020 - January 24, 2021*, pp. 7139–7145.
- [3] M. Saveriano and D. Lee, “Learning barrier functions for constrained motion planning with dynamical systems,” in *Proceedings of IEEE/RSJ International Conference on Intelligent Robots and Systems, IROS, Macau, SAR, China, November 3-8, 2019*, pp. 112–119.
- [4] T. A. Howell, B. E. Jackson, and Z. Manchester, “ALTRO: A fast solver for constrained trajectory optimization,” in *IEEE/RSJ International Conference on Intelligent Robots and Systems, IROS, Macau, SAR, China, November 3-8, 2019*, pp. 7674–7679.
- [5] M. Kelly, “An introduction to trajectory optimization: How to do your own direct collocation,” *SIAM Review*, vol. 59, no. 4, pp. 849–904, 2017.
- [6] B. Thananjeyan, A. Balakrishna, S. Nair, M. Luo, K. Srinivasan, M. Hwang, J. E. Gonzalez, J. Ibarz, C. Finn, and K. Goldberg, “Recovery RL: safe reinforcement learning with learned recovery zones,” *IEEE Robotics Automation Letters*, vol. 6, no. 3, pp. 4915–4922, 2021.
- [7] A. D. Ames, J. W. Grizzle, and P. Tabuada, “Control barrier function based quadratic programs with application to adaptive cruise control,” in *Proceedings of 53rd IEEE Conference on Decision and Control, CDC, Los Angeles, CA, December 15-17, 2014*, pp. 6271–6278.
- [8] Q. Nguyen, A. Hereid, J. W. Grizzle, A. D. Ames, and K. Sreenath, “3d dynamic walking on stepping stones with control barrier functions,” in *Proceedings of 55th IEEE Conference on Decision and Control, CDC, Las Vegas, NV, December 12-14, 2016*, pp. 827–834.
- [9] T. Gurriet, A. Singletary, J. Reher, L. Ciarletta, E. Feron, and A. D. Ames, “Towards a framework for realizable safety critical control through active set invariance,” in *Proceedings of 9th ACM/IEEE International Conference on Cyber-Physical Systems, ICCPS, Porto, Portugal, April 11-13, 2018*, pp. 98–106.
- [10] J. J. Choi, D. Lee, K. Sreenath, C. J. Tomlin, and S. L. Herbert, “Robust control barrier-value functions for safety-critical control,” in *Proceedings of 60th IEEE Conference on Decision and Control, CDC, Austin, TX, December 14-17, 2021*, pp. 6814–6821.
- [11] A. Robey, H. Hu, L. Lindemann, H. Zhang, D. V. Dimarogonas, S. Tu, and N. Matni, “Learning control barrier functions from expert demonstrations,” in *Proceedings of 59th IEEE Conference on Decision and Control, CDC, Jeju Island, South Korea, December 14-18, 2020*, pp. 3717–3724.
- [12] H. Ma, B. Zhang, M. Tomizuka, and K. Sreenath, “Learning differentiable safety-critical control using control barrier functions for generalization to novel environments,” *CoRR*, vol. abs/2201.01347, 2022.
- [13] J. Rawlings, “Tutorial overview of model predictive control,” *IEEE Control Systems Magazine*, vol. 20, no. 3, pp. 38–52, 2000.
- [14] J. Kong, M. Pfeiffer, G. Schildbach, and F. Borrelli, “Kinematic and dynamic vehicle models for autonomous driving control design,” in *Proceedings of IEEE Intelligent Vehicles Symposium, Seoul, South Korea, June 28 - July 1, 2015*, pp. 1094–1099.
- [15] A. Herdt, N. Perrin, and P. Wieber, “Walking without thinking about it,” in *Proceedings of IEEE/RSJ International Conference on Intelligent Robots and Systems, IROS, Taipei, Taiwan, October 18-22, 2010*, pp. 190–195.
- [16] M. Neunert, M. Stäuble, M. Gifthaler, C. D. Bellicoso, J. Carius, C. Gehring, M. Hutter, and J. Buchli, “Whole-body nonlinear model predictive control through contacts for quadrupeds,” *IEEE Robotics and Automation Letters*, vol. 3, no. 3, pp. 1458–1465, 2018.
- [17] A. D. Ames, S. Coogan, M. Egerstedt, G. Notomista, K. Sreenath, and P. Tabuada, “Control barrier functions: Theory and applications,” in *Proceedings of 17th European Control Conference, ECC, Naples, Italy, June 25-28, 2019*, pp. 3420–3431.
- [18] M. Lutter, C. Ritter, and J. Peters, “Deep lagrangian networks: Using physics as model prior for deep learning,” in *7th International Conference on Learning Representations, ICLR, New Orleans, LA, May 6-9, 2019*.
- [19] S. Lucia, A. Tătulea-Codrean, C. Schoppmeyer, and S. Engell, “Rapid development of modular and sustainable nonlinear model predictive control solutions,” *Control Engineering Practice*, vol. 60, pp. 51–62, 2017.
- [20] Y. Emam, P. Glotfelter, Z. Kira, and M. Egerstedt, “Safe model-based reinforcement learning using robust control barrier functions,” *CoRR*, vol. abs/2110.05415, 2021.
- [21] M. Aicardi, G. Casalino, A. Bicchi, and A. Balestrino, “Closed loop steering of unicycle like vehicles via lyapunov techniques,” *IEEE Robotics Automation Magazine*, vol. 2, no. 1, pp. 27–35, 1995.